1.

2. Received Date: 13-Jan-2016

3. Accepted Date: 25-Aug-2016

4. Article Type: Original Article

5. Groundwater shapes sediment biogeochemistry and microbial diversity in a submerged Great Lake sinkhole

6. Lauren E. Kinsman-Costello[1], Cody S. Sheik[2], Nathan Sheldon[3], G. Allen Burton[4], David Costello[1], Daniel Marcus[5], Paul Den Uyl[6], and Gregory Dick[3]

7. [1]Department of Biological Sciences, Kent State University; [2]Large Lakes Observatory, University of Minnesota Duluth; [3]Department of Earth and Environmental Sciences, University of Michigan; [4]School of Natural Resources and the Environment, University of Michigan; [5]Department of Microbiology & Biophysics, The Ohio State University; [6]The Research Corporation of the University of Hawaii

8. Corresponding Author: Lauren Kinsman-Costello

9. Details for Corresponding author

a. Department of Biological Sciences, Kent State University, PO Box 5190, Kent, OH 44242-0001

b. lkinsman@kent.edu

c. Phone: 330-672-3640; Fax: 330-672-3713

Groundwater shapes sediment biogeochemistry and microbial diversity in a submerged Great Lake sinkhole

Abstract

For a large part of earth's history, cyanobacterial mats thrived in low oxygen conditions, yet our understanding of their ecological functioning is limited. Extant cyanobacterial mats provide windows into the putative functioning of ancient ecosystems, and they continue to mediate biogeochemical transformations and nutrient transport across the sediment-water interface in modern ecosystems. The structure and function of benthic mats are shaped by biogeochemical processes in underlying sediments. A modern cyanobacterial mat system in a submerged sinkhole of Lake Huron (LH) provides a unique opportunity to explore such sediment-mat interactions. In the Middle Island Sinkhole (MIS), seeping groundwater establishes a low-oxygen, sulfidic environment in which a microbial mat dominated by *Phormidium* and *Planktothrix* that is capable of both anoxygenic and oxygenic photosynthesis, as well as chemosynthesis, thrives. We explored the coupled microbial community composition and biogeochemical functioning of organic-rich, sulfidic sediments underlying the surface mat. Microbial communities were diverse and vertically stratified to 12 cm sediment depth. In contrast to previous studies, which used low-throughput or shotgun metagenomic approaches, our high throughput 16S rRNA gene sequencing approach revealed extensive diversity. This diversity was present within microbial groups, including putative sulfate-reducing taxa of *Deltaproteobacteria*, some of which exhibited differential abundance patterns in the mats and with depth in the underlying sediments. The biological and geochemical conditions in the MIS were distinctly different from those in typical LH sediments of comparable depth. We found evidence for active cycling of sulfur, methane, and nutrients leading to high concentrations of sulfide, ammonium, and phosphorus in sediments underlying cyanobacterial mats. Indicators of nutrient availability were significantly related to MIS microbial community composition, while LH communities were also shaped by indicators of subsurface groundwater influence. These results show that interactions between the mats and sediments are crucial for sustaining this hotspot of biological diversity and biogeochemical cycling.

Introduction

In the distant past, cyanobacteria-dominated microbial mats were the dominant forms of life, and are believed to have flourished in low-oxygen environments lacking multicellular grazers and herbivores (Bertrand *et al.* 2015). Cyanobacterial mat metabolic activity shaped biogeochemical cycles in the Precambrian and drove major turning points in the geochemical evolution of Earth's surface (Hoehler, Bebout & Des Marais 2001; Hayes & Waldbauer 2006). Although mats in coastal oceans are often assumed to be the agents of such global change, recent work suggests that terrestrial and freshwater cyanobacterial mats may have played a critical role in Earth's oxygenation (Lalonde & Konhauser 2015). Under certain conditions, benthic mats proliferate on the sediment surface in modern aquatic ecosystems (Stal 1995), where they are powerful engineers of ecosystem condition and biogeochemical function (Canfield & Des Marais 1993; Paerl, Pinckney & Steppe 2000). In these modern, sometimes extreme, environments, mat consortia provide insight into how living organisms shape the biogeochemistry of our planet, both now and in the distant past (Paerl *et al.* 2000; Sumner *et al.* 2015).

Benthic microbial mat communities are tightly linked to the microbial communities in underlying sediments. Photosynthetic mats stabilize surface sediments (Decho 1990) and exude labile organic substrates, which in turn fuel heterotrophic microbial metabolism, establishing physicochemical gradients of oxygen concentration, pH, and redox potential. These sharp gradients are strengthened and maintained by the physical structure of mat communities, which slows molecular diffusion and prevents movement of particles across the sediment-water interface (Stal 1995; Paerl *et al.* 2000). Together these physical and chemical effects of microbial mats influence biogeochemical cycling, especially the mobility of metals and nutrients across the sediment-water interface (Battin *et al.* 2003; Nimick *et al.* 2003). Sediments beneath microbial mats, which are typically organic-rich, serve as a reservoir and source of nutrients that fuel mat growth and function, a role that may be especially important to mats that live in low-nutrient waters (Bertrand *et al.* 2015). When disturbance from grazing and bioturbating animals is limited, resources supplied from underlying sediment may be the dominant control over mat structure and function.

In the absence of oxygen, the sediment environment supports alternative terminal electron accepting process, such as iron and sulfate (SO_4^{2-}) reduction, fermentation, and methanogenesis (Schlesinger & Bernhardt 2013). Byproducts of complex organic matter

breakdown and fermentation fuel SO_4^{2-} reducing microorganisms (Megonigal, Hines & Visscher 2004), and in turn the sulfide produced can then be used to drive two forms of primary production: anoxygenic photosynthesis and sulfide oxidation (Voorhies *et al.* 2012; Bertrand *et al.* 2015). Methanogenesis in deep organic sediments provides an energy source for methanotrophic organisms, supports carbon breakdown in anoxic environments that lack other terminal electron acceptors, and produces a highly potent greenhouse gas (Megonigal *et al.* 2004; Schlesinger & Bernhardt 2013). Despite the importance of sediment microbial communities and geochemistry, underlying sediments are often overlooked when characterizing benthic microbial mat ecosystems.

Submerged groundwater seeps in karst sinkholes of the Laurentian Great Lakes establish chemically distinct ecosystems \where unique benthic microbial mat communities thrive (Biddanda *et al.* 2009). Low oxygen, high sulfate, brackish groundwater seeps into sinkholes in Lake Huron near Alpena, MI (Ruberg *et al.* 2005, 2008), which contain lush microbial mats of filamentous cyanobacteria and sulfur-oxidizing bacteria (Biddanda *et al.* 2006; Ruberg *et al.* 2008; Nold *et al.* 2010a). In the 23-m deep Middle Island Sinkhole (MIS, Fig. 1), the sulfidic, anoxic conditions and low-level irradiance (~5%) support a metabolically flexible cyanobacterial mat community dominated by relatives of *Phormidium autumnale* and members of the genus *Planktothrix* (Nold *et al.* 2010a; Voorhies *et al.* 2012).

As a whole, the MIS mat community is capable of high rates of primary production by a combination of oxygenic photosynthesis, anoxygenic photosynthesis, and chemosynthetic sulfide oxidation (Voorhies *et al.* 2012). Beneath the cyanobacterial mat, the sinkhole is filled with organic-rich sediment (Nold *et al.* 2013) that supports a diverse microbial community (Nold *et al.* 2010a; Nold, Zajack & Biddanda 2010b). Preliminary research by Nold et al. (2010a, 2010b) indicated SO_4^{2-} reduction and methanogenesis in MIS sediments, as well as diverse and active benthic bacterial sediment communities. However, our understanding of this benthic diversity remains limited by the shallow sediment depth sampled (2 cm) and by the number of taxa detected using clone library techniques. For example, none of the clones retrieved were related to known SO_4^{2-} reducing bacteria (Nold *et al.* 2010a), despite the known importance of SO_4^{2-} reduction in the system. To explore the role of underlying sediments in MIS benthic ecosystem functioning and assess vertical stratification of sediment community structure and function more broadly, we sampled sediment cores (0–12 cm) from within the MIS and from a similar depth

and substrate texture in a nearby non-sinkhole area of Lake Huron (LH, Fig. 1). We find that sinkhole sediment microbial communities are diverse, and change with depth through the sediment-water interface and into deep sediments along geochemical gradients that both reflect and shape microbial community function.

Methods

Site Description

The MIS (45° 11.914 N, 83° 19.671 W) consists of an approximately 1-hectare sinkhole and groundwater seep at 23 m depth in LH near Alpena, MI (Fig. 1; Ruberg *et al.* 2008). Brackish (specific conductivity = 2300 $\mu S\ cm^{-1}$) groundwater carrying salts dissolved from water-rock reactions between groundwater and ~400 million year old Detroit River Group (Middle Devonian) limestones and evaporites (Ruberg *et al.* 2008) flows from an adjacent seep (the "alcove") and spills into the MIS. Seeping groundwater forms an approximately meter-thick "lens" of higher density water above the sediment water interface that resists mixing with the surrounding fresh LH water (200 $\mu S\ cm^{-1}$), establishing a distinct ecosystem bounded by this chemocline (Ruberg *et al.* 2008). Although irradiance conditions change seasonally at this latitude, other physicochemical characteristics are relatively consistent in the MIS groundwater layer. Specific conductivity, dissolved oxygen, pH, and temperature are relatively stable at 1700 $\mu S\ cm^{-1}$, 2–4 mg L^{-1}, 7–7.5, and 9.5–12 °C, respectively (Ruberg *et al.* 2008). In comparison, these conditions vary seasonally in overlying Lake Huron water as would be expected in a large freshwater lake (Ruberg *et al.* 2008, unpublished data).

Sediment Sample Collection and Processing

Scuba divers collected sediment cores from the MIS on five dates in June 2011, September 2011, September 2012, May 2013, and July 2013. Microbial community composition and geochemical characteristics were measured in vertically-stratified samples from cores collected on all dates. Pore water was also sampled and geochemically characterized from cores sampled in September 2012, May 2013, and July 2013. In May 2013, divers also collected sediment cores from a non-sinkhole location nearby in LH (45° 12.333 N, 83° 19.850 W) of comparable water depth for simultaneous measurement of microbial community composition, sediment geochemistry, and pore water geochemistry. Divers inserted 20 × 7 cm (length × inner diameter) clear polycarbonate tubes through surface mat material and into soft sediments to

obtain an intact core preserving the vertical structure of benthic overlying water, mat, and 12–15 cm of sediment.

Cores collected in June and September 2011 were frozen within 24 hours of collection and later divided by sawing into vertical sections (water chemistry was not measured for the frozen samples). Cores collected on September 2012, May 2013, and July 2013 were transported upright and on ice in the dark to Ann Arbor, MI, where they were stored at 4 °C in the dark for up to 48 hours. For each of these three sampling events, four replicate cores were sampled and processed by first removing overlying water, then removing surface mat material, and finally dividing each core into vertical sections (3 cm). In September 2012, pore water was sampled from pre-drilled holes using an 18 gauge needle and filtered through 0.45 µm filters (PVDF, Thermo Scientific). In May and July 2013, pore water was sampled from pre-drilled holes at the vertical mid-point of 3 cm sections using soil moisture samplers (Rhizon, Rhizosphere Research Products) with a nominal pore size of 0.2 µm. Pore waters were extracted using syringes attached to Rhizon samplers with three-way valves, creating a closed system that prevented loss of methane gas during sampling. All pore water samples were analyzed for nutrients, major ions, and methane gas. Replicate cores were extruded vertically from the polycarbonate tube and sectioned at 3 ± 0.5 cm intervals for geochemical characterization of sediments. In July 2013, three additional cores were processed such that the top 3 cm of sediment were sectioned vertically into three 1-cm aliquots to be subsampled for microbial community composition and sediment geochemistry. Pore water was sampled at 3 cm intervals, as above. When necessary for statistical analyses, the pore water value measured for the top (0-3 cm) sediment section was related to the solid phase geochemical measurement or microbial community composition of each of the top three 1 cm segments. Due to limited solid material, mat material was sometimes pooled across replicate cores within season for geochemical characterization.

In September 2012, benthic overlying water chemistry was assessed in surface water siphoned from cores. We observed minimal variability among replicate cores (e.g., across 6 cores Cl^- concentrations ranged from 21-31 mg/L and averaged 27 mg/L, with a standard deviation of 3.8 mg/L). On future sampling dates, benthic overlying water samples were collected by divers using a syringe to obtain water as close to the mat-water interface as possible without causing disturbance. On July 2013, divers collected water venting directly from the

adjacent groundwater seep for water chemistry analysis. We measured sediment bulk density in sediment samples taken in May and July 2013.

Microsensor Measurements

Hydrogen sulfide (H_2S) and oxygen (O_2) concentrations were measured at fine vertical resolution using microsensors in intact cores from the MIS collected in September 2011 and July 2013 within 12 hours of collection. Cores were stored upright on ice in a dark cooler between collection and microsensor profiling at room temperature under ambient indoor light. Amperometric microsensors for O_2 and H_2S (Unisense, 100 µm tip size; Revsbech 1989, Jeroschewski *et al.* 1996) were calibrated according to manufacturers instructions immediately before profiling. Briefly, the O_2 microelectrode was calibrated with a two point curve that included air saturated water and an anoxic solution of 0.1 M sodium ascorbate (in 0.1 M NaOH). The H_2S microelectrode was calibrated with a linear standard curve that covered a H_2S concentration range of 0–5 mM (Na_2S in pH 4 buffer). After each profile, the calibration of the microsensors was verified with a calibration standard and a new curve was prepared if necessary (required for H_2S only). Simultaneous profiling of O_2 and H_2S in cores was done using a micromanipulator (Unisense) after aligning the two sensor tips horizontally at the surface of the water in the core. Starting in the overlying water above the mat and sediment, O_2 and H_2S were measured at 500 µm vertical intervals through the mat–water interface until the sensor tip was 2–3 cm into the sediment (Kühl & Revsbech 2001). Within each core, we completed 2–4 replicate profiles, each in a different location on the surface of the core. Because pH was not measured concurrently, the data presented here is only the H_2S fraction of total sulfide.

Chemical Analyses

Cation (NH_4^+, Ca^{2+}, Mg^{2+} and Na^+) and major anion (SO_4^{2-}, NO_3^-, Cl^-) concentrations were quantified using membrane-suppression ion chromatography (Dionex, Thermo Scientific), soluble reactive phosphate (PO_4^{3-}) concentrations using the molybdate blue colorimetric method (Murphy & Riley 1962), and dissolved methane concentrations using gas chromatography with a flame ionization detector (Hewlett Packard, Tekmar). Total manganese (Mn), iron (Fe), and phosphorus (P) were extracted using microwave assisted digestion (MARS) with a mixture of nitric and hydrochloric acid and quantified with inductively coupled plasma optical emission

spectroscopy (PerkinElmer Optima 8000). Sediment organic matter content was quantified two ways; 1) loss on ignition (LOI) and 2) measuring total organic C and N content using samples decarbonated in weak (2%) HCl, dried, and weighed (~5 mg) into solvent-rinsed tin capsules and then combusted in a Costech ECS4010 elemental analyzer. External precision was maintained at better than 0.1% for both C and N and results were calibrated against a certified acetanilide standard (C = 71.09%, N = 10.36%).

Acid volatile sulfides (AVS) in sediments were quantified using the US EPA Method 821-R-91-100 (Allen *et al.* 1991). Briefly, frozen sediment subsamples were acidified (1M HCl) and released sulfide was captured in an alkaline solution (0.5 M NaOH). Total AVS was quantified colorimetrically with a mixed diamine reagent (H_2SO_4, N,N-dimethyl-p-phenylenediamine oxalate, and ferric chloride hexahydrate). Analytical sulfide standards were prepared from a stock solution (prepared and kept anaerobic under a headspace of N_2 gas) and standardized against a thiosulfate stock solution.

Microbial Community Composition Methods

DNA extraction, quantification, amplification and Illumina amplicon sequencing

Bulk DNA was extracted from 0.5 g (wet weight) sediment using the FastDNA Spin kit for soil (MP Biomedical, Santa Anna, CA, USA) following the manufacturer's protocol with the exception of using 0.3 g of beads. Total extracted DNA was quantified with PicoGreen (Invitrogen, Carlsbad, CA, USA). 16S rRNA genes were PCR amplified with primers (515F-806R) (Bates *et al.* 2011) that contained dual index barcodes and Illumina MiSeq specific adapters (Kozich *et al.* 2013). PCRs consisted of 10 μ of HotMasterMix (5prime, Gaithersburg, MD, USA), 12 μ (of PCR grade water (Ambion, Life Technologies, Grand Island, NY, USA), 1 μ each of forward and reverse primer (10 SA), 1 A), μ e of DNA. Reaction conditions were: 94 °C for 4 min followed by 30 rounds of 94 °C for 30 sec, 50 °C for 45 sec, 72 °C for 1 min and a final extension step of 72 °C for 10 min. For each sample, triplicate 25 μ o PCRs were done then pooled prior to cleaning. Pooled PCR samples were cleaned using the UltraClean PCR cleanup kit (MoBio, Carlsbad, CA, USA). Pooled PCRs were quantified with Picogreen (Invitrogen), combined into a single sample at near equivalent concentrations and sent for 2×250 sequencing with the Illumina MiSeq platform at the University of Michigan's Microbial Systems Core

Sequencing facility. Sequences may be obtained from NCBI Sequence Read Archive (SRA-SRP067517).

OTU clustering, data analysis and statistics

OTUs were clustered using a modified Uparse pipeline (Edgar 2013). With Uparse, Illumina paired sequence reads (iTags) were joined (flags: –fastq_mergepairs) and filtered and length truncated (flags: -fastq_filter, -fastq_maxee 1.0, and –fastq_trunclen 250). iTags were dereplicated with an in-house perl script (available at github.com/Geo-omics/scripts), sorted, then operational taxonomic units (OTUs) were clustered at a 0.97 cutoff. OTUs were classified to the Silva v.111 taxonomy (Pruesse *et al.* 2007) with the naive Bayesian classifier (Wang et al. 2007) in Mothur (v 1.31) (Schloss *et al.* 2009). A phylogenetic tree of representative OTU sequences (with chloroplasts and mitochondria omitted) was calculated with FastTree (Price, Dehal & Arkin 2009). Using the R statistical environment (R Core Team 2015), an OTU table was rarefied to a uniform depth (13,000 iTags per sample) and phylogenetic diversity (PD) (Faith 1992) was calculated with Picante (Kembel *et al.* 2010). Prior to ordination calculation, the OTU abundances were normalized with DESeq (Anders and Huber 2010), as suggested by McMurdie and Holmes (2014). Nonmetric multidimensional scaling (NMDS) plots were calculated with Bray-Curtis dissimilarities using the metaMDS function (autotransformation=F, binary=F).

We used ANOSIM to test for significant differences in OTU community composition between LH sediment, MIS mat, and MIS sediment (Clarke 1993). To test for differences between MIS and LH and for changes in parameters along vertical gradients, we used linear mixed effects models. The models use an ANCOVA design, predicting response variables (geochemical parameters or microbial relative abundance data at different taxonomic levels) from the fixed effects of location (categorical), depth into sediments (continuous), and the interaction between them. Random effects of sample date and intact core identity were included in these mixed effects models to account for variability associated with these factors.

To assess relationships between sediment microbial community composition and geochemical characteristics, we conducted Mantel tests comparing dissimilarity matrices based on normalized prokaryotic OTU reads (Bray-Curtis distance) and sediment pore water and geochemical characteristics (Euclidean distance). We first compared community composition to the entire suite of geochemical characteristics to assess the overall relationship between sediment

geochemistry and microbial community composition in each of the two locations, MIS and LH. Due to incomplete data across samples, sediment LOI and AVS were omitted from these "whole-suite" analyses, and pore water CH_4 was omitted from the LH analysis. After omitting sediment samples with incomplete geochemical data, 11 and 34 samples from LH and MIS were tested, respectively. We also used Mantel tests to assess relationships between microbial community composition differences and differences among individual geochemical variables. Within all groups of results, significance values (alpha = 0.05) were corrected for multiple comparisons (Benjamini & Hochberg 1995). Unless stated otherwise, values are stated as means ± standard deviation.

Results

Solid Phase Sediment Geochemistry

Geochemically, sediments from MIS and LH demonstrated many qualitative and quantitative differences (Table 1). Sediments from MIS were darker, finer, and less dense than the sandier LH sediments. MIS sediments contained significantly more organic matter than LH sediments, when measured as total organic C, total organic N, and LOI (Table 1, Table 2). In both MIS and LH sediments, organic C and N decreased with depth and C:N ratio increased with depth (Table 2). Low organic N led to high C:N ratios in LH sediments (Table 2).

Sediment total Fe, total Mn, and total P concentrations were generally higher in MIS sediments than LH sediments (Table 1). In MIS, total Fe increased significantly with depth into sediments (Table 1–2). In contrast, total Fe decreased with depth in LH sediments (Table 1–2). Sediment total P significantly decreased with depth in both MIS and LH sediments (Table 1–2). Phosphorus was more concentrated in the surface mat material than sediments below (Table 1). In MIS sediments, AVS did not change significantly with depth, although concentrations were more variable in surface sediments than in deeper sediments (Table 1). Averaged across depths, MIS AVS concentrations (67 ± 25 µmol S g^{-1} n=23), were an order of magnitude higher than AVS concentrations in LH sediments (6.4 ± 3.5 µmol S g^{-1}; n=3).

Benthic and Pore Water Geochemistry

Biologically reactive solutes (SO_4^{2-}, NH_4^+, PO_4^{3-}, and CH_4) displayed steep vertical gradients in MIS sediments, and also changed with depth in LH sediments, but at lower concentrations (Fig. 2, Table 2). In contrast, more conservative ions (Ca^{+2}, Mg^{+2}, Na^+, and Cl^-),

294 which are indicators of groundwater influence, did not change significantly with depth in MIS
295 sediments, but increased with depth in LH sediment cores, reflecting likely subsurface
296 groundwater influence. Ammonium and PO_4^{3-} both increased significantly with depth into MIS
297 sediments to much higher concentrations than in deep LH sediments (Fig. 2, Table 2). Pore water
298 NO_3^- concentrations in MIS were uniformly low (1.5 ± 1.5 µM) and did not change significantly
299 with depth into sediments (Table 2, Fig. 2). In contrast, LH benthic waters contained
300 measureable concentrations of NO_3^- (20 ± 2.5 µM), which decreased significantly with depth
301 (Table 2, Fig. 2) to 1.2 ± 0.1 µM. The source groundwater seeping into the MIS from the
302 "alcove" contained low nutrient concentrations: 13 µM NO_3^-, 9 µM NH_4^+, and 1 µM PO_4^{3-}
303 (Ruberg *et al.* 2008).
304 Sulfate concentrations in benthic water overlying MIS mats were 7.1 ± 1.5 mM, much
305 higher than in LH (0.2 ± 0.04 mM), reflecting input from the MIS groundwater seep (11 mM
306 SO_4^{2-}, Fig. 2). Sulfate concentrations significantly decreased with depth into MIS sediments,
307 from 4.5 ± 2.2 mM in the top 0–3 cm of sediments to 0.5 ± 0.5 mM in the bottom 9–12 cm of
308 sediments (Fig. 2,Table 2). Conversely, SO_4^{2-} concentrations in LH sediments increased with
309 depth, 0.8 ± 0.5 in the top 0–3 cm to 5.4 ± 0.8 mM in the bottom 6–9 cm (Fig. 2,Table 2).
310 Microsensor measurements of intact MIS sediment cores revealed that O2 concentrations
311 decrease to below detection within 1–3 cm into the sediments (Fig. 3). Hydrogen sulfide was
312 detected within the surface mat, and increased with depth to high concentrations of 1–7 mM
313 within the top 0–3 cm of sediments, and in some profiles, showed no evidence of leveling off at
314 this depth (Fig. 3). Hydrogen sulfide concentrations in pore waters vary considerably across
315 space and season (Fig. 3). The apparent co-occurrence of H_2S and O_2 in some profiles is likely
316 due to artifacts either from a "hole effect" produced by the relatively deep profiles and/or rapid
317 sensor measurements that were not allowed to equilibrate to accurate measurements. However,
318 the general patterns of O_2 depletion and H_2S increase with depth illustrated by these data are
319 robust, and measurement artifacts do not invalidate the conclusion that the mats represent net
320 sinks of O_2 and net sources of sulfide. In fact, our measurements likely underestimate of O_2 and
321 H_2S fluxes. In addition, although we did not measure pH and thus sulfide concentrations are
322 presented as only the H_2S fraction of total hydrogen sulfide, the general patterns are unlikely to
323 change with pH correction.

Methane concentrations in sediment pore waters and overlying benthic waters were higher in MIS than LH sediments (Fig. 2). In MIS sediment pore waters, CH_4 concentrations increased significantly with depth (Fig. 2, Table 2), but there was considerable temporal variability. Methane concentrations were highest in July and September (63-2030 µM range) and lowest in May (37-223 µM range). Across seasons, MIS CH_4 concentrations tended to be highest at mid-depths (3–6 cm; 521 ± 603 µM), with slightly lower concentrations in deeper and shallower sediments (0-3cm: 183 ± 147 µM; 6–9 cm: 321 ± 314 µM; 9–12cm: 395 ± 273 µM). Concentrations of CH_4 in deep LH sediments were much lower (2.5 ± 0.3 µM).

Microbial Community Composition

We detected 14,127 unique microbial operational taxonomic units (OTUs) across 114 total samples. Over a third of all OTUs (5,290) were detected in every sample type: MIS mats, MIS sediments, and LH sediment (Figure S1). Only 103 OTUs were unique to MIS mats, and these were all detected at low abundance (<122 reads). Most high-abundance OTUs were either shared among all three groups, or were shared between MIS mats and MIS sediments but absent from LH sediments (Fig. S1–S2). Of the OTUs detected, 174 were classified as mitochondria or chloroplasts. Whole-community composition patterns were similar whether OTUs classified as chloroplasts and mitochondria were included or omitted from the analysis (Fig. S3). We detected OTUs representing 53 phyla of *Bacteria*. More *Archaea* were detected in sediments than in MIS surface mats and all archaeal OTUs detected were classified as belonging to the phylum *Euryarchaeota* (Fig. 4).

Despite the large number of shared OTUs, the structure of microbial communities in MIS sediment and mat samples were distinctly different from those in LH sediments (ANOSIM, R = 0.73, p=0.001, Fig. 5). MIS microbial mats were dominated by *Cyanobacteria*, whereas underlying MIS sediments were dominated by *Bacteriodetes* and *Proteobacteria* (Table S1, Fig. 4). Lake Huron sediments had fewer *Bacteriodetes* and more *Nitrospirae* than MIS sediments (Fig. 4). LH sediment communities displayed less variability among samples than among MIS samples (Fig. 5). MIS mat communities overlapped somewhat with MIS sediment communities (Fig. 5). Microbial community composition changed with depth into sediments in both MIS and LH (Fig. 5). In MIS, 18 of the 19 major microbial groups changed significantly with depth ($p<0.05$), whereas only six of the 19 changed significantly with depth in LH sediment cores (Fig. 6).

Cyanobacterial mat community

95 of the 380 OTUs classified as *Cyanobacteria* were chloroplasts, including several of the high relative abundance OTUs. The most abundant of these (OTU_2) was classified as a relative of the diatom *Odontella sinensis,* but with only 22% maximum likelihood. Other OTUs identified as chloroplasts were similar to sequences without meaningful taxonomic information. The four non-chloroplast *Cyanobacteria* OTUs with high average relative abundance (>1%) in the MIS surface mat samples were representatives of the genera *Phormidium* (OTU_1, OTU_3202) and *Planktothrix* (OTU_7, OTU_2819). The two high-abundance *Phormidium* OTU's, OTU 1 and OTU 3202, were 100% and 98% similar, respectively, in sequence to a dominant *Phormidium* previously detected in MIS mats (Voorhies *et al.* 2012). Although *Plantktothrix* (formerly called *Oscillatoria*) has traditionally been found in pelagic environments, it has been found both in MIS mats and cyanobacterial mat communities in other sulfidic environments (Klatt *et al.* 2015, Camancho *et al.* 2000, Voorhies *et al.* 2012). In LH sediments, the only OTUs classified as *Cyanobacteria* with meaningful relative abundances were chloroplasts. Mat communities and surface sediments contained other evidence of eukaryotes in abundant mitochondria (e.g., OTU_28) and an amoeba symbiont (OTU_107).

Putative sulfate reducing bacteria

We detected OTUs classified to five orders containing known SO_4^{2-} reducing bacteria (SRB): *Desulfarculales*, *Desulfobacteriales*, *Desulfovibrionales*, *Desulfurellales*, and *Desulfuromonadales*. All high relative abundance putative SRB were phylogenetically related to members of the *Desulfobacterales*. Two putative SRB, OTU_3 and OTU_9, were among the most abundant non-*Cyanobacteria* OTUs across all samples. The most abundant putative SRB in the surface mats, OTU_3, was phylogenetically classified (maximum likelihood=100) as a filamentous SO_4^{2-} reducer in the genus *Desulfonema* also detected in the Frasassi cave system (ACC No. DQ133916, Macalady et al. 2006). Relative abundances of this OTU decreased with depth (Fig. 7) in the MIS, and were very low in LH sediments. The other high abundance OTU (OTU_9) was classified as a member of the genus *Desulfocapsa*, and also showed highest abundance in mats with decreasing abundance with depth into MIS sediments (Fig. 7) and very low abundance in LH sediments. *Desulfocapsa* can disproportionate elemental sulfur and thiosulfate (Finster, Liesack & Thamdrup 1998).

In contrast to these putative SRB OTUs with highest relative abundance in MIS surface mats, several putative SRB increased with depth into MIS sediments (Fig. 7). An OTU classified to the genus *Desulfatirhabdium* (OTU_13) was the most abundant putative SRB in sediments beneath the MIS surface mat. The only named species in this genus oxidizes butyrate and reduces sulfur (Balk *et al.* 2008). The most abundant putative SRB in LH sediments (OTU_41) was classified to the genus of the SVa0081 sediment group. This OTU was also detected at lower abundances in MIS sediments and mats (0.15% and 0.04%, respectively), and did not change with depth in MIS or LH.

Putative sulfur oxidizers

Relative abundances of putative sulfide oxidizers of the *Epsilonprotoeobacteria* and *Beggiatoa* sp. relatives were higher in MIS communities than in LH sediments (Fig. 4, Table S1). Similar to the putative SRBs, putative sulfide oxidizing OTUs showed variable vertical patterns with depth into sediments. OTUs related to *Sulfurospirillum* (OTU_19), *Helicobacteraceae* (OTU_33), and *Beggiatoa* (OTU_4) were detected at highest relative abundance in surface mat material and decreased with depth into sediments (Figure S4). In contrast, relatives of *Sulfuricurvum* (OTU_14192 and OTU_22), and another *Sulfurospirillum* (OTU_18), had higher relative abundance in underlying MIS sediments, with some evidence for a peak at intermediate depths (3–6 cm; Figure S4).

Euryarchaeota

All *Euryarchaeota* taxa tended to increase in relative abundance with depth into the sediments. Of the 1248 OTUs classified in the Phylum *Euryarchaeota*, only 21 were identified as putative methanogens (18 OTUs in the *Methanomicrobia*, 3 OTUs in the *Methanobacteria*). Putative methanogens were highest in abundance in deep MIS sediments, detected at much lower relative abundance in LH sediments, and exceedingly low in abundance or not detected in MIS surface mats. Two putative methanogens, OTU_117 and OTU_252, of the genus *Methanosaeta* and *Methanoregula*, respectively, dominated the methanogenic community of MIS sediments.

Other high-abundance sediment *Euryarchaeota* OTUs were related to *Halobacteria* and *Thermoplasmota*. Of the four classes to which *Euryarchaeota* OTUs were classified, deep sea hydrothermal vent *Halobacteria* (1145 OTUs) represented the highest relative abundance in sediments, followed by *Thermoplasmata* (82 OTUs). Most archaeal OTUs were associated with members of the uncultured *Woesearchaeota* (formerly DHVEG-6). Two *Woesearchaeota* OTUs,

OTU_84 and OTU_85, were among the highest abundance archaeal OTUs and showed nearly identical patterns within cores, increasing with depth in MIS sediments, and virtually undetected in LH sediments and MIS surface mat material.

Putative methanotrophs

We detected 30 OTUs classified as aerobic *Gammaproteobacteria Methylococcales*, although at low relative abundances (0–0.34%). *Methylococcales* OTU relative abundances were highest at intermediate sediment depths (2–5 cm) on average. We did not detect any OTUs allied with members of the NC10 phylum (denitrifying methanotrophs), despite the high concentrations of methane detected in pore waters. Only one detected OTU (OTU_11930) had low phylogenetic similarity to known archaeal anaerobes that pair methane oxidization to sulfate reduction (ANME-1). This OTU was detected only in 10 deep (>5 cm) sediment samples at very low relative abundance (0.0003–0.004%).

Microbial community composition significantly correlated to geochemical gradients

Differences in microbial community composition among samples were significantly related to their geochemical differences in both MIS (r_{Mantel} = 0.5439, p = 0.001, n = 34) and LH sediments (r_{Mantel} = 0.7761, p = 0.002, n =11). Specifically, MIS community differences were significantly related to differences in multiple indicators of nutrient availability, including pore water PO_4^{3-} and NH_4^+ concentrations, and sediment organic C, organic N, LOI, total Fe and total P (Table 3). LH sediment community differences were also significantly related to some nutrient availability indices (PO_4^{3-}, NH_4^+, Organic C, Organic N), but indices of groundwater influence (concentrations of SO_4^{2-}, Cl^-, Na^+, Ca^{2+}, and Mg^{2+}) also strongly predicted community differences (Table 3).

Discussion

Great Lakes submerged sinkholes contain diverse microbial communities shaped by low-oxygen, brackish groundwater (Biddanda *et al.* 2009; Nold *et al.* 2010a,b) that may provide insights into the microbial ecology and biogeochemistry of ancient ecosystems. By deeply sequencing the microbial community at multiple sediment depths in the MIS in parallel with extensive geochemical characterization of pore water and sediment nutrient concentrations, we have expanded our understanding of this unique ecosystem. The results presented here indicate that the MIS ecosystem is geochemically and biologically distinct from the surrounding freshwater benthic system of Lake Huron, and that it is highly vertically stratified through the

photosynthetic and chemosynthetic surface mat and into the high-nutrient sediments below, where sulfur and methane cycling become dominant.

The sinkhole ecosystem is distinct

We compared biogeochemical conditions in the MIS to a reference location in LH of similar depth. Despite evidence of groundwater upwelling at the LH site based on conservative ions (Fig. 2), benthic conditions within the MIS and at the LH "control" site are vastly different. In the MIS, groundwater venting out of an adjacent seep that spills and settles into the sinkhole establishes a benthic ecosystem with stable physicochemical conditions (with the exception of light, which changes seasonally) that rarely mixes with overlying freshwater (Ruberg *et al.* 2008), creating distinct geochemical and ecological conditions at the sediment-water interface. In comparison, despite apparent groundwater influence at LH, the sediment-water interface reflects the chemistry of seasonally variable, low conductivity LH waters (Sanders *et al.* 2011).

At coarse and fine taxonomic levels, the biotic communities of the MIS and LH sediments differ greatly. Despite the presence of many shared OTU sequences among MIS and LH samples, microbial communities of the MIS sediments are starkly different than communities of LH sediments when considering relative abundances (Figs. 5–7). Although deeper LH sediments experience groundwater influence, the microbial community of these sediments was still more similar to that of shallow LH sediments than any MIS sinkhole sample. As expected, we observed vertically stratified microbial communities in sediments from both ecosystems, although it was most pronounced in MIS. Vertical stratification occurs not only at the level of major taxonomic groups, but also at the level of individual OTUs within taxonomic and functional groups (Figs. 5–7). Overall, MIS microbial community composition at the OTU level was stratified by relationships with nutrients and redox chemistry, while LH communities were more related to gradients in conservative indicators of groundwater influence (Tables 1–2) (although we cannot rule out that these geochemical measurements are indicative of other correlated factors that we did not measure). These differences between sites illustrate the importance of groundwater influence at the sediment-water interface in establishing the unique community of the MIS, both in the microbial mat and in underlying sediments.

Nutrient-rich sediments

Despite experiencing light conditions that are presumably similar to the MIS, LH sediment cores contained no visible surface microbial mat, and no molecular evidence of

478 *Cyanobacteria* was detected. It seems that the chemical environment established by venting
479 groundwater in the MIS allows microbial mat communities to establish, in part by relieving
480 grazing pressure due to low dissolved oxygen concentrations (Stal 1995). The MIS microbial mat
481 is capable of high primary production rates (Voorhies *et al.* 2012), yet underlying sediments
482 largely reflect isotopic characteristics of settling phytoplankton (Nold *et al.* 2013), implying
483 rapid decomposition of mat biomass prior to burial (Canfield & Des Marais 1993) and/or
484 significant upward mat motility (Biddanda *et al.* 2015) to avoid burial.
485 Surface microbial mats in the MIS are surrounded by low-nutrient overlying water, and
486 thus likely depend on inorganic nutrients diffusing up from pore waters for growth.
487 Concentrations of dissolved nutrients in the MIS pore waters are remarkably higher than in non-
488 sinkhole LH sediments. In addition, MIS sediments contain more solid organic material than
489 typical LH sediments, and the material is of higher nutrient quality (lower C:N ratio). The high
490 nutrient nature of the MIS sediments is likely due to a combination of abiotic environmental
491 conditions established by venting groundwater and biotic microbial community effects. The low
492 oxygen environment of the sinkhole likely slows decomposition of settling particles, establishing
493 sediments containing a higher proportion of organic matter than surrounding "typical" Lake
494 Huron sediments.
495 Although microbial mat biomass is often rapidly, and sometimes completely,
496 decomposed before burial (Canfield & Des Marais 1993), mats likely play direct and indirect
497 roles in establishing and maintaining high-nutrient conditions of underlying sediment material,
498 further enhancing the high-nutrient conditions encouraged by the low oxygen environment. The
499 mats may play a direct role in sediment nutrient conditions through their motility, which allows
500 them to physically bury organic particles (Stal 1995; Biddanda *et al.* 2015). In addition, their
501 extracellular polysaccharide matrix can slow diffusion of nutrient molecules and limit re-
502 suspension of particles into overlying waters (Decho 1990). Mat cyanobacteria may further
503 prevent loss of valuable nutrients to benthic overlying water by sequestering nutrients within
504 their biomass through luxury uptake and storage (Kromkamp 1987. Molecular evidence reveals
505 that the dominant MIS surface mat cyanobacteria *Phormidium* genome encodes phycobilisome
506 proteins (Voorhies *et al.* 2016), pigments that can be plentiful in cyanobacteria (Bogorad 1975)
507 and are degraded by cells experiencing N stress (Luque *et al.* 2001), implying a role as N storage
508 molecules. In comparison, although LH sediments likely receive comparable nutrient inputs from

settling pelagic material, the higher-oxygen environment there likely leads to nutrient loss as particles are more rapidly decomposed.

Sulfur cycling

The influence of high-SO_4^{2-} groundwater in the MIS establishes an ecosystem that contains much more sulfur than typical freshwater ecosystems. Combined with anoxic conditions and abundant organic matter, this provides ideal conditions for microbial SO_4^{2-} reduction, resulting in high concentrations of sulfide, a portion of which is sequestered as AVS by binding with Fe and other metals. Despite high sulfur concentrations in the MIS habitat, microbial community composition was not statistically related to the geochemical indicators of sulfur cycling that we measured (SO_4^{2-}, AVS). Our bulk sediment sampling resolution was relatively coarse (3 cm) and it is possible that sulfur gradients drive microbial diversity over smaller spatial scales. In addition, it is likely that SO_4^{2-} concentrations are so uniformly high that community composition is structured by other controllers of SO_4^{2-} reduction, like the availability of carbon and/or electron donors such as low molecular weight organic substrates and/or hydrogen. Even in the deepest sediments sampled (12 cm), measureable SO_4^{2-} was often detected, implying that in shallow sediments, SO_4^{2-} reduction is not limited by SO_4^{2-} availability. Regardless, microbes of the MIS sediments must be adapted to the remarkably high sulfide concentrations we measured below the mat-water interface. Hydrogen sulfide is highly toxic to most forms of aerobic life, diminishes the bioavailability and toxicity of divalent metals (Di Toro *et al.*, 1990, Hansen *et al.*, 2005), and can also serve as an energy source for chemosynthetic microbes (Schlesinger & Bernhardt 2013). Thus, particularly at high concentrations, sulfide can strongly shape ecosystem structure and function (Kinsman-Costello *et al.* 2015).

Despite the lack of broad relationships with geochemical indicators of sulfur, taxonomic markers indicate a diverse sulfur cycling microbial community in the MIS. Previous studies based on clone libraries of MIS mat and shallow sediments detected a single *Epsilonproteobacteria* and no relatives of known SRBs (Nold *et al.* 2010a). This study broadens our view of putative sulfur cycling microbial diversity in sediments. Surface mat and sediment communities both contained OTUs related to known SO_4^{2-}-reducing members of the *Deltaproteobacteria* in the *Desulfobacterales* (238 OTUs) as well as members of the sulfide-oxidizing *Epsilonproteobacteria Campylobacterales* (45 OTUs) and relatives of sulfur-oxidizing members of the genus *Beggiatoa* (14 OTUs). Metagenomic and metatranscriptomic work on

MIS mat material has detected expression of known SO_4^{2-}-reduction genes in association with a *Desulfobacterales* genomic bin, and known sulfide-oxidation genes associated with a *Campylobacterales* bin (Voorhies, 2014), further strengthening the evidence that members of these groups shape sulfur cycling in the sediments below as well.

Contrasting patterns of relative abundance with depth observed for putative SRB OTUs suggests niche partitioning of SO_4^{2-} reduction in this high-SO_4^{2-} environment. Although all of the notable SRB OTUs identified in the MIS and LH were members of the *Desulfobacterales*, individual OTUs displayed contrasting patterns of relative abundance. While some *Desulfobacterales* were enriched in the MIS mat, others increased in relative abundance with depth into the sediments, and some were only detected at meaningful relative abudance in LH sediments. Future work elaborating on physiological differences of OTUs that are present and functioning in different vertical zones may provide valuable information of how SO_4^{2-} supports MIS heterotrophy. Evidence continues to emerge that SO_4^{2-} reduction is not limited to specific redox zones as classically thought (Froelich *et al.* 1979), but can be mediated by physiologically diverse organisms in a range of environments and redox conditions (Canfield & Des Marais 1991; Hansel *et al.* 2015). The high SO_4^{2-} levels present at MIS make this a valuable system in which to explore the diversity of SO_4^{2-} reduction processes and organisms.

Methane Cycling and Archaea Diversity

A picture of the MIS is emerging as a dynamic CH_4 producer and consumer. Pore water CH_4 concentrations, although higher than concentrations measured in LH pore waters, were lower than concentrations (~20 mM) previously measured in deep sediments at the MIS (Nold *et al.* 2010a). Differences in CH_4 concentrations from previous studies may be in part due to differences in sampling techniques that influence the inclusion or exclusion of gas bubbles in pore water samples. Regardless, this and previous studies demonstrate that methane concentrations in MIS decrease in shallower sediments and benthic overlying water, implying CH_4 consumption by methanotrophs in upper sediment layers and mat material. Metagenomic and –transcriptomic work detected expression of a gene for CH_4 oxidation (mmoC) associated with a *Gammaproteobacteria Methylococcales* bin (Voorhies, 2014). Although we detected OTUs allied with the aerobic *Methylococcales* only at low relative abundances, declining CH_4 concentrations in shallow anoxic sediments suggest anaerobic CH_4 oxidation. Given the high availability of SO_4^{2-}, we expected to detect evidence for members of the ANME clades that pair

571 CH_4 oxidation with SO_4^{2-} reduction (Boetius *et al.* 2000), yet we detected only a single OTU
572 allied with the ANME-1 present at very low relative abundance in a handful of samples. Thus,
573 our understanding of the MIS methanotrophic community remains limited, and it is likely that
574 currently unknown organisms oxidize methane in this system.
575 MIS sediments contained an archaeal community distinct from that in LH. We detected a
576 diverse array of OTUs at high relative abundance allied with *Woesearchaeota* and
577 *Thermoplasmata* at high relative abundance. Relatives of these OTUs were virtually undetected
578 in LH sediments, implying that these *Archaea* are a distinct feature of sediments of submerged
579 sinkhole ecosystems and not common in typical freshwater sediments. The physiological and
580 metabolic functions of the DHVEG-6 group at MIS remain unknown, although members of this
581 group have been detected in numerous anaerobic environments including the subsurface, saline
582 and hypersaline lakes and deep sea methane seep sediments (Castelle *et al.* 2015, Kuroda *et al.*
583 2015, and citations therein). Recent metagenomic analysis suggests that some members of this
584 phylum have highly reduced genomes and are specialized for a fermentative lifestyle (Castelle *et*
585 *al.* 2015).

586 ***Conclusions***

587 Using deep microbial community sequencing and parallel geochemical characterization,
588 we reveal a diverse and biogeochemically dynamic sediment ecosystem underlying benthic
589 microbial mats in the MIS. In combination with data from a nearby site devoid of mat, these
590 results provide insights into both how geochemistry promotes mat growth at MIS, and how the
591 MIS mats influence sediment geochemistry. In this Great Lakes submerged sinkhole, a vertically
592 stratified microbial community mediates sulfur and methane cycling in a high-nutrient
593 environment, setting the stage for the metabolically flexible surface mat above to conduct a
594 mixture of anoxygenic photosynthesis, oxygenic photosynthesis, and chemosynthetic sulfur
595 oxidation. These results highlight the geobiological influence of microbial mats in promoting
596 high nutrient flux from sediments to surface mats, establishing a positive feedback that would
597 enhance primary productivity of microbial mats in ancient ecosystems. Future research
598 investigating magnitudes of and controls on process rates in this distinct ecosystem will enhance
599 our understanding of its tightly linked biogeochemistry, the causes and effects of microbial
600 diversity, and potential biomarkers for detecting similar systems earlier on in Earth's history.
601 Such studies have high potential to provide insight into the functioning and co-evolution of

microbial communities in low-oxygen microbial mat ecosystems both now and in the distant past.

Acknowledgements

We are especially grateful to the NOAA Thunder Bay National Marine Sanctuary for their support in field site access and sampling, in particular to the dive team including Russ Green, Tane Casserly, Joe Hoyt, Wayne Lusardi, Cathy Green, and Stephanie Gandulla, and ship captains Mike Taesch, Steve Bawks, and Beau Breymer. Bopi Biddanda, Michael Snider, Kathryn Gallagher, Adam McMillan, and Chelsea Mervenne assisted with field sampling, sample processing, and laboratory analyses. Special thanks to Tim Gallagher and Katy Rico for assistance in total organic C and N analysis. We gratefully acknowledge the lab of Dr. Steve Hamilton at Michigan State University, in particular David Weed, for providing facilities and support for ion chromatography analysis. Thanks to Tom Yavarski and the University of Michigan EWRE Aquatic Biology Lab for facilities and support in methane analysis. Funding was generously provided by the University of Michigan MCubed program and NSF grant EAR-1035955 to G.J.D. and N.D.S.

Works Cited

Allen HE, Fu G., Boothman W, DiToro DM, Mahoney JD (1991) Determination of acid volatile sulfides (AVS) and simultaneously extracted metals in sediment: Draft analytical method for determination of acid volatile sulfide in sediment. Washington, DC: U.S. Environmental Protection Agency.

Balk M, Altinbaş M, Rijpstra WIC, Damsté JSS, Stams AJM (2008) *Desulfatirhabdium butyrativorans* gen. nov., sp. nov., a butyrate-oxidizing, sulfate-reducing bacterium isolated from an anaerobic bioreactor. *International Journal of Systematic and Evolutionary Microbiology* **58**, 110–115.

Battin TJ, Kaplan LA, Newbold DJ, Hansen CME (2003) Contributions of microbial biofilms to ecosystem processes in stream mesocosms. *Nature* **426**, 439–442.

Bates ST, Berg-Lyons D, Caporaso JG, Walters WA, Knight R, Fierer N (2011) Examining the

global distribution of dominant archaeal populations in soil. *The ISME Journal* **5**, 908-917.

Benjamini Y, Hochberg Y (1995) Controlling the false discovery rate: A practical and powerful approach to multiple testing. *Journal of the Royal Statistical Society. Series B (Methodological)* **57**, 289–300.

Bertrand J-C, Caumette P, Lebaron P, Matheron R (2015) *Environmental Microbiology: Fundamentals and Applications*. (eds Bertrand J-C, Caumette P, Lebaron P, Matheron R, Normand P, Sime-Ngando T), Springer, Netherlands.

Biddanda BA, Coleman DF, Johengen TH. Ruberg SA, Meadows GA, Van Sumeren HW, Rediske RR, Kendall ST (2006) Exploration of a submerged sinkhole ecosystem in Lake Huron. *Ecosystems* **9**, 828–842.

Biddanda BA, McMillan AC, Long SA, Snider MJ, Weinke AD (2015) Seeking sunlight: rapid phototactic motility of filamentous mat-forming cyanobacteria optimize photosynthesis and enhance carbon burial in Lake Huron's submerged sinkholes. *Frontiers in Microbiology* **6**, 1–13.

Biddanda BA, Nold SC, Ruberg SA, Kendall ST, Sanders TG & Gray JJ (2009) Great Lakes Sinkholes: A Microbiogeochemical Frontier. *EOS, Transactions, American Geophysical Union* **90**, 62–69.

Boetius A, Ravenschlag K, Schubert CJ, Rickert D, Widdel F, Gieseke A, Amann R, Jørgenson BB, Witte U, Pfannkuche O (2000) A marine microbial consortium apparently mediating anaerobic oxidation of methane. *Nature* **407**, 623–626.

Bogorad L (1975) Phycobiliprotein: complementary chromatic adaptation. *Annual Review of Plant Physiology.* **26**, 369–401.

Camacho A, Vicente E, Miracle MR (2000) Ecology of a deep-living *Oscillatoria (=Planktothrix)* population in the sulphide-rich waters of a Spanish karstic lake. *Archiv fur Hydrobiologie* **148**, 333-355.

Canfield DE, Des Marais DJ (1991) Aerobic sulfate reduction in microbial mats. *Science* **251**, 1471–1473.

Canfield DE, Des Marais DJ (1993) Biogeochemical cycles of carbon, sulfur, and free oxygen in

a microbial mat. *Geochimica et cosmochimica acta* **57**, 3971–3984.

Castelle CJ, Wrighton KC, Thomas BC, Hug LA, Brown CT, Wilkins MJ, Frischkorn KR, Tringe SG, Singh A, Markillie LM, Taylor RC, Williams KH, Banfield JF (2015) Genomic expansion of domain archaea highlights roles for organisms from new phyla in anaerobic carbon cycling. *Current Biology* **25**, 690-701.

Decho AW (1990) Microbial exopolymer secretions in ocean environments: Their role(s) in food webs and marine processes. *Oceanography and Marine Biology Annual Review* **28**, 73–153.

Di Toro DM, Mahony JD, Hansen DJ, Scott KJ, Hicks MB, Mayr SM, Redmond MS (1990) Toxicity of cadmium in sediments: The role of acid volatile sulfide. *Environmental Toxicology and Chemistry* **9**:1487–1502.

Edgar RC (2013) UPARSE: highly accurate OTU sequences from microbial amplicon reads. *Nature Methods* **10**, 996–998.

Faith DP (1992) Conservation evaluation and phylogenetic diversity. *Biological Conservation* **61**, 1–10.

Finster K, Liesack W, Thamdrup B (1998) Elemental sulfur and thiosulfate disproportionation by Desulfocapsa sulfoexigens sp. nov., a new anaerobic bacterium isolated from marine surface sediment. *Applied and environmental microbiology* **64**, 119–125.

Froelich PN, Klinkhammer GP, Bender ML, Luedtke NA, Heath GR, Cullen D, Dauphin P (1979) Early oxidation of organic matter in pelagic sediments of the eastern equatorial Atlantic: suboxic diagenesis. *Geochimica et Cosmochimica Acta* **43**, 1075–1090.

Hansel CM, Lentini CJ, Tang Y, Johnston DT, Wankel SD & Jardine PM (2015) Dominance of sulfur-fueled iron oxide reduction in low-sulfate freshwater sediments. *The ISME Journal*, 1–13.

Hansen D, Di Toro DM, Berry W, Boothman W, McGrath J, Ankley GT (2005) Procedures for the derivation of equilibrium partitioning sediment benchmarks (ESBs) for the protection of benthic organisms: Metal mixtures (cadmium, copper, lead, nickel, silver and zinc). EPA 600/R-02/011. US Environmental Protection Agency, Washington, DC.

Hayes JM, Waldbauer JR (2006) The carbon cycle and associated redox processes through time.

Philosophical Transactions of the Royal Society B: Biological Sciences **361**, 931–950.

Hoehler TM, Bebout BM, Des Marais DJ (2001) The role of microbial mats in the production of reduced gases on the early Earth. *Nature* **412**, 324–327.

Jeroschewski P, Steuckart C, Kühl M (1996) An amperometric microsensor for the determination of H_2S in aquatic environments. *Analytical Chemistry* **68,** 4351-4357.

Kembel SW, Cowan PD, Helmus MR, Cornwell WK, Morlon H, Ackerly DD, Blomberg SP, Webb CO (2010) Picante: R tools for integrating phylogenies and ecology. *Bioinformatics* **26**, 1463–1464.

Kinsman-Costello LE, O'Brien JM, Hamilton SK (2015) Natural stressors in uncontaminated sediments of shallow freshwaters: The prevalence of sulfide, ammonia, and reduced iron. *Environmental Toxicology and Chemistry* **34**, 467–479.

Klatt JM, Haas S, Yllmaz P, de Beer D, Polerecky L (2015) Hydrogen sylfide can inhibit and enhance oxygenic photosynthesis in a cyanobacterium from sulfidic springs. *Environmental Microbiology* **17**, 3301-3313.

Kozich JJ, Westcott SL, Baxter NT, Highlander SK, Schloss PD (2013) Development of a dual-index sequencing strategy and curation pipeline for analyzing amplicon sequence data on the MiSeq Illumina sequencing platform. *Applied and Environmental Microbiology* **79**, 5112–5120.

Kromkamp J (1987) Formation and functional significance of storage products in cyanobacteria. *New Zealand Journal of Marine and Freshwater Research* **21**, 457–465.

Kühl M, Revsbech NP (2001) Biogeochemical microsensors for boundary layer studies. In: *The Benthic Boundary Layer.* (eds Boudrew BP, Jørgensen BB), p 180-210. Oxford University Press, New York, NY, USA.

Kuroda K, Hatamoto M, Nakahara N, Abe K, Takahashi M, Araki N, Yamaguchi T (2015) Community composition of known and uncultured archaeal lineages in anaerobic or anoxic wastewater treatment sludge. *Microbial Ecology* **69**, 586–596.

Lalonde SV, Konhauser KO (2015) Benthic perspective on Earth's oldest evidence for oxygenic photosynthesis. Proceedings of the National Academy of Sciences, USA **112**, 995-1000.

716 Luque I, Zabulon G, Contreras A, Houmard J (2001) Convergence of two global transcriptional
717 regulators on nitrogen induction of the stress-acclimation gene nblA in the cyanobacterium
718 *Synechococcus* sp. PCC 7942. *Molecular microbiology* **41**, 937–47.

719 Macalady JL, Lyon EH, Koffman B, Albertson LK, Meyer K, Galdenzi S, Mariani S (2006)
720 Dominant microbial populations in limestone-corroding stream biofilms, Frasassi cave
721 system, Italy. *Applied and Environmental Microbiology* **72**, 5596–5609.

722 McMurdie PJ, Holmes S (2014) Waste not, want not: Why rarefying microbiome data is
723 inadmissible. *PLoS Computational Biology* **10**, e1003531.

724 Megonigal JP, Hines ME, Visscher PT (2004) Anaerobic metabolism: Linkages to trace gases
725 and aerobic processes. *Biogeochemistry*, 317–424.

726 Murphy J, Riley JP (1962) A modified single solution method for the determination of phosphate
727 in natural waters. *Analytica Chimica Acta* **27**, 31–36.

728 Nimick DA, Gammons CH, Cleasby TE, Madison JP, Skaar D, Brick CM (2003) Diel cycles in
729 dissolved metal concentrations in streams: Occurrence and possible causes. *Water*
730 *Resources Research* **39**, 1247.

731 Nold SC, Bellecourt MJ, Kendall ST, Ruberg SA, Sanders TG, Klump JV, Biddanda BA (2013)
732 Underwater sinkhole sediments sequester Lake Huron's carbon. *Biogeochemistry* **115**, 235–
733 250.

734 Nold SC, Pangborn JB, Zajack HA, Kendall ST. Rediske RR, Biddanda BA (2010a) Benthic
735 bacterial diversity in submerged sinkhole ecosystems. *Applied and Environmental*
736 *Microbiology* **76**, 347–351.

737 Nold SC, Zajack HA, Biddanda BA (2010b) Eukaryal and archaeal diversity in a submerged
738 sinkhole ecosystem influenced by sulfur-rich, hypoxic groundwater. *Journal of Great Lakes*
739 *Research* **36**, 366–375.

740 Paerl HW, Pinckney JL, Steppe TF (2000) Cyanobacterial-bacterial mat consortia: Examining
741 the functional unit of microbial survival and growth in extreme environments.
742 *Environmental Microbiology* **2**, 11–26.

743 Price MN, Dehal PS, Arkin AP (2009) FastTree: Computing large minimum evolution trees with

profiles instead of a distance matrix. *Molecular Biology and Evolution* **26**, 1641–1650.

Pruesse E, Quast C, Knittel K, Fuchs BM, Ludwig W, Peplies J, Glöckner FO (2007) SILVA: a comprehensive online resource for quality checked and aligned ribosomal RNA sequence data compatible with ARB. *Nucleic Acids Research* **35**, 7188–7196.

R Core Team (2015) R: A languate and environment for statistical computing. R Foundation for Statistical Computing, Vienna, Austria. URL https://www.R-project.org/

Revsbech NP (1989) An oxygen microsensor with a guard cathod. *Limnology & Oceanography* **34**, 474-478.

Ruberg SA, Coleman DF, Johengen TH. Meadows GA, Van Sumeren HW, Lang GA, Biddanda BA (2005) Groundwater plume mapping in a submerged sinkhole in Lake Huron. *Marine Technology Society Journal* **39**, 65–69.

Ruberg SA, Kendall ST, Biddanda BA, Black T, Nold SC, Lusardi WR, Green R, Casserly Tane, Smith E, Sanders TG, Lang GA, Constant SA (2008) Observations of the Middle Island Sinkhole in Lake Huron – A unique hydrogeologic and glacial creation of 400 million years. *Marine Technology Society Journal* **42**, 12–21.

Sanders TGJ, Biddanda BA, Stricker CA, Nold SC (2011) Benthic macroinvertebrate and fish communities in Lake Huron are linked to submerged groundwater vents. *Aquatic Biology* **12**, 1–12.

Schlesinger WH, Bernhardt ES (2013) *Biogeochemistry: An Analysis of Global Change*, 3rd edn. Academic Press, Waltham, MA.

Schloss PD, Westcott SL, Ryabin T, Hall JR, Hartmann M, Hollister EB, Lesniewski RA, Oakley BB, Parks DH, Robinson CJ, Sahl JW, Stres B, Thallinger GG, Van Horn DJ, Weber CF (2009) Introducing mothur: Open-source, platform-independent, community-supported software for describing and comparing microbial communities. *Applied and Environmental Microbiology* **75**, 7537–7541.

Stal LJ (1995) Tansley Review No. 84 Physiological ecology of cyanobacteria in microbial mats and other communities. *New Phytologist* **131**, 1–32.

Sumner DY, Hawes I, Mackey TJ, Jungblut AD, Doran PT (2015) Antarctic microbial mats: A

772 modern analog for Archean lacustrine oxygen oases. *Geology* **43**, 887–890.

773 Voorhies AA, Biddanda BA, Kendall ST, Jain S, Marcus DN, Nold SC, Sheldon ND, Dick GJ
774 (2012) Cyanobacterial life at low O_2: Community genomics and function reveal metabolic
775 versatility and extremely low diversity in a Great Lakes sinkhole mat. *Geobiology* **10**, 250–
776 267.

777 Voorhies AA (2014) Investigation of microbial interactions and ecosystem dynamics in a low O2
778 cyanobacterial mat. Doctoral dissertation, University of Michigan.

779 Voorhies AA, Eisenlord SD, Marcus DN, Duhaime MB, Biddanda BA, Cavalcoli JD, Dick GJ
780 (2016) Ecological and genetic interactions between cyanobacteria and viruses in a low-
781 oxygen mat community inferred through metagenomics and metatranscriptomics.
782 *Environmental Microbiology* **18**, 358-371.

783

Table 1. Solid phase characteristics of sediments collected from the Middle Island Sinkhole (MIS Sed) and a nearby non-sinkhole location in Lake Huron (LH Sed) of similar depth, and cyanobacterial mat material from the sinkhole (MIS Mat). Data are from cores collected in September 2012 (MIS), May 2013 (MIS and LH), and July 2013 (MIS). Values are means plus or minus standard deviation.

Location	Depth (cm)	n†	Bulk Density (g cm^{-3})	Loss on Ignition (%)	Organic C (%)	Organic N (%)	Molar C:N	Total Mn (μmol g^{-1})	Total Fe (μmol g^{-1})	Total P (μmol g^{-1})	AVS (μmol g^{-1})
MIS Mat		4	nm	28.4±7.9[3]	11.3±0.8[4]	1.6±0.1[4]	8.2±0.1	2.9±0.5	164±33	92±39	nm
MIS Sed	1.9±0.2	12	0.2±0.08[1]	10.7±4.7	8.6±2.7	1.1±0.4	8.9±0.4	3.6±0.7	235±11	31±.5.8	85±48[5]
	5±0.1	12	0.26±0.10[1]	7.4±1.9	6.4±1.5	0.8±0.2	9.5±0.5	4.3±1.0	224±29	24±4.1	58±19[5]
	8±0.2	11	0.26±0.05[1]	7.9±1.5	6.4±0.9	0.8±0.1	9.4±0.3	4.5±0.8	255±15	23±2.5	64±23[5]
	11.2±0.3	11	0.38±0.14[2]	7.7±1.4	6.2±0.9	0.8±0.1	9.5±0.5	4.5±0.9	271±16	22±2.2	60±7[5]
LH Sed	1.5±0	4	0.8±0.44	3.0±0.2	2.1±0.3	0.3±0.02	10.1±0.4	3.8±1.1	175±30	16±2.3	8[6]
	4.5±0.1	4	0.88±0.14	1.7±0.2	1.0±0.2	0.1±0.01	12.4±1.8	2.8±0.6	157±27	14±3.1	9[6]
	6.9±0.2	4	0.52±0.21	1.8±1.4	0.6±0.1	0.1±0.02	13.8±1.5	2.0±0.4	123±25	11±1.6	2[6]

nm = not measured

† Sample size (number of replicate cores), unless otherwise noted.

[1]n=8; [2]n=7; [3]n=5, [4]n=7, [5]n=3, [6]n=1

Table 2. Results (p values) of mixed effects models (except where noted) testing the effects of location (Middle Island Sinkhole, MIS, vs. Lake Huron, LH) and depth into sediments (MIS Slope, LH Slope) on geochemical characteristics, accounting for the random effects of sample date and intact core (not shown). Significant ($p<0.05$, after Benjamini and Hochberg (1995) correction) terms are in bold. Detailed statistical results are shown in supplemental materials (Table S2). For significant slopes, the sign of the relationship is indicated in parentheses, with (+) indicating that the parameter increases with depth into sediments and (-) indicating a decreases with depth into sediments.

	df†	MIS Slope	MIS vs. LH	LH Slope
Pore water chemistry				
SO_4^{2-}	54	**<0.001 (-)**	**0.002**	**<0.001 (+)**
NH_4^+	54	**<0.001 (+)**	**<0.001**	0.915
NO_3^-	57	0.064	**<0.001**	**0.007** (-)
SRP	55	**<0.001 (+)**	**<0.001**	0.405
CH_4	46	**<0.001 (+)**	**<0.001**	0.067
Ca^{2+}	54	0.956	**<0.001**	**<0.001 (+)**
Mg^{2+}	54	**0.020 (+)**	**<0.001**	**<0.001 (+)**
Na^+	53	0.667	**<0.001**	**<0.001 (+)**
Cl^-	54	0.140	**0.031**	**<0.001 (+)**
Sediment Geochemistry				
Loss on Ignition	35	**0.001**	**0.001**	0.765
Organic C	50	**<0.001** (-)	**<0.001**	**<0.001** (-)
Organic N	50	**<0.001 (-)**	**<0.001**	**<0.001** (-)
C:N molar ratio	50	**<0.001 (+)**	0.41	**<0.001 (+)**
Total Mn	44	**<0.001 (+)**	0.395	**<0.001** (-)
Total Fe	44	**0.002 (+)**	0.178	**<0.001** (-)
Total P	44	**<0.001** (-)	**<0.001**	0.432
AVS*	11	0.569	0.026	0.151

*Acid Volatile Sulfide, linear model testing the fixed effects of Depth and Location on the response variable (measured in both MIS and LH, but not on multiple TimeIDs)

† Residual degrees of freedom

Table 3. Results of Mantel tests, including sample size (n), Mantel statistic (r_M), and significance (p), of Mantel tests for relationships between microbial community pairwise distances (Bray-Curtis) and geochemical variable pairwise distances (Euclidean) among samples collected from the Middle Island Sinkhole (MIS) and a site of similar depth in Lake Huron (LH). Due to low sample size, the relationship between AVS and LH community composition was not assessed. Relationships with $r_M > 0.5$ are in bold.

	MIS			**LH**		
Water Chemistry	n	r_M	p*	n	r_M	p*
SRP	58	**0.581**	**0.002**	11	**0.519**	**0.038**
NH_4^+	58	**0.603**	**0.002**	11	**0.555**	**0.013**
NO_3^-	58	0.028	0.318	11	0.097	0.243
SO_4^{2-}	58	0.018	0.388	11	**0.791**	**0.002**
Cl^-	58	0.148	0.049	11	**0.762**	**0.003**
Na^+	57	0.016	0.406	11	**0.752**	**0.003**
Ca^{2+}	58	0.029	0.309	11	**0.684**	**0.002**
Mg^{2+}	58	-0.003	0.486	11	**0.777**	**0.002**
Sediment Chemistry						
Organic C	96	**0.548**	**0.002**	11	**0.582**	**0.003**
Organic N	96	**0.530**	**0.002**	11	**0.604**	**0.002**
Loss on Ignition	42	**0.782**	**0.002**	7	0.209	0.130
Total Fe	47	**0.520**	**0.002**	11	0.294	0.049
Total P	47	**0.766**	**0.002**	11	0.475	0.014
Total Mn	47	0.289	0.003	11	**0.643**	**0.002**
AVS	22	0.122	0.224	NA		

*Corrected for multiple comparisons (Benjamini and Hochberg 1995)

Figure Legends

Fig. 1. (A) Map depicting location of submerged sinkhole research area in Lake Huron and geologic map of bedrock aquifers (modified from Ruberg et al. 2008; Biddanda et al. 2009), (B) Map illustrating Middle Island Sinkhole sampling location and nearby Lake Huron "control" site of similar depth and substrate (Map data: Google, NOAA, 2015 TerraMetrics).

Fig. 2. Mean concentrations (± 1 standard deviation) of dissolved solutes in overlying benthic and sediment pore water in the Middle Island Sinkhole (MIS), nearby Lake Huron sediments (LH), compared with concentrations in groundwater at the "alcove," the major seep feeding the MIS (GW) and overlying surface Lake Huron water (LHO). The dashed line indicates the sediment-water interface, with positive depth values denoting vertical distance below the sediment-water interface. MIS values represent means of pore water concentrations measured in four replicate cores on each of September 2012, May 2013, and July 2013 (n = 16), whereas LH values represent means of four replicate cores sampled only on May 2013.

Fig. 3. Microelectrode measured vertical profiles of dissolved oxygen (O_2, open circles) and hydrogen sulfide (H_2S, filled circles) in representative intact cores sampled from the Middle Island Sinkhole in September 2011 (A) and July 2013 (B). The gray rectangle indicates the approximate location of the sediment-water interface, with positive depth values denoting vertical distance below the sediment-water interface. Points represent averages of 2–4 replicate profiles with standard deviation bars. Elevated oxygen concentrations above the sediment-water interface may be laboratory artifacts due to oxygen diffusion through overlying water during core handling and processing.

Fig. 4. Average relative abundance of OTUs categorized into major groups across samples of Middle Island Sinkhole mat material (MIS Mat, n = 17), MIS underlying sediments (MIS Sed, n = 87: 0–3 cm n = 31; 3–6 cm n = 17; 6–9 cm n = 22; >9 cm n = 17), and non-sinkhole Lake Huron sediments (LH Sed, n = 11). Summary relative abundances of major groups in MIS Sediment, LH Sediment, and MIS mat samples are tabulated in Table S1.

Fig. 5. Non-metric multidimensional scaling ordination of microbial communties in microbial mat and sediment material collected from the Middle Island Sinkhole (Sinkhole Mat and Sinkhole Sediment, respectively) in Lake Huron, MI and in sediment material collected in a nearby non-sinkhole area of Lake Huron at comparable depth (Lake Huron Sediment). Points are shaded by depth into the sediment, with 0 representing the sediment-water interface, and higher numbers reflected depth (in cm) below the sediment-water interface.

Fig. 6. Degree of change with depth into sediments of relative abundance of major microbial groups in the Middle Island Sinkhole (A, MIS) and Lake Huron sediments (B, LH). Points to the left of the vertical 0-line represent major groups that decreased with relative abundance with depth into sediments, and points to the right represent groups that increased with depth. Change with depth is the slope of the relationship between arcsine-square root transformed major group relative abundance and depth into sediments (with zero being the sediment-water interface, and surface mats assigned a value of -1 cm) as modeled by a mixed effects model accounting for the random effects of sampling date and intact core. Significance levels are based on p-values corrected for multiple comparisons using the Benjamini and Hochberg correction. Major microbial groups represented at least 1% relative abundance in MIS surface mats, MIS sediments, or LH sediments.

Fig. 7. Relative abundance of OTUs taxonomically associated with known sulfate-reducing bacteria detected in DNA sequenced from Middle Island Sinkhole surface mat material (MIS Mat) and underlying organic sediments (MIS Sed) in comparison with sandy Lake Huron sediments from comparable depth (LH Sed) plotted versus depth into sediments, with "0" denoting the sediment-water interface. All OTUs are classified as members of the *Deltaproteobacteria*. Based on the finest level of classification with maximum likelihood greater than 90, OTUs are classified as: A) OTU 9, uncultured *Desulfocapsa*; B) OTU 3, uncultured *Desulfonema* with 100% maximum likelihood classification as a filamentous sulfate reducer also found in limestone-corroding biofilms from the Frasassi caves (AccNo DQ133916, Macalady et al. 2006); C) OTU 26, uncultured *Desulfobacteraceae*, D) OTU 13, uncultured *Desulfatirhabdium*, E) OTU9739, uncultured *Desulfobacteraceae*, F) OTU 41, uncultured *Desulfobacteraceae* related to a Genus of the SVa0081 sediment group (AccNo AB630779)

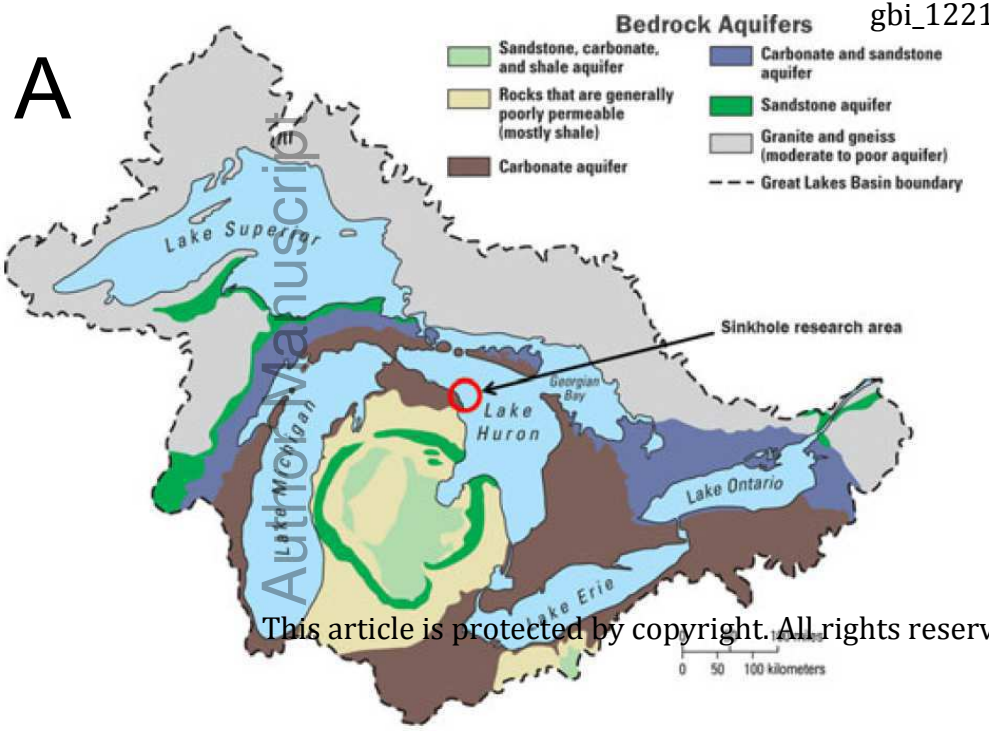

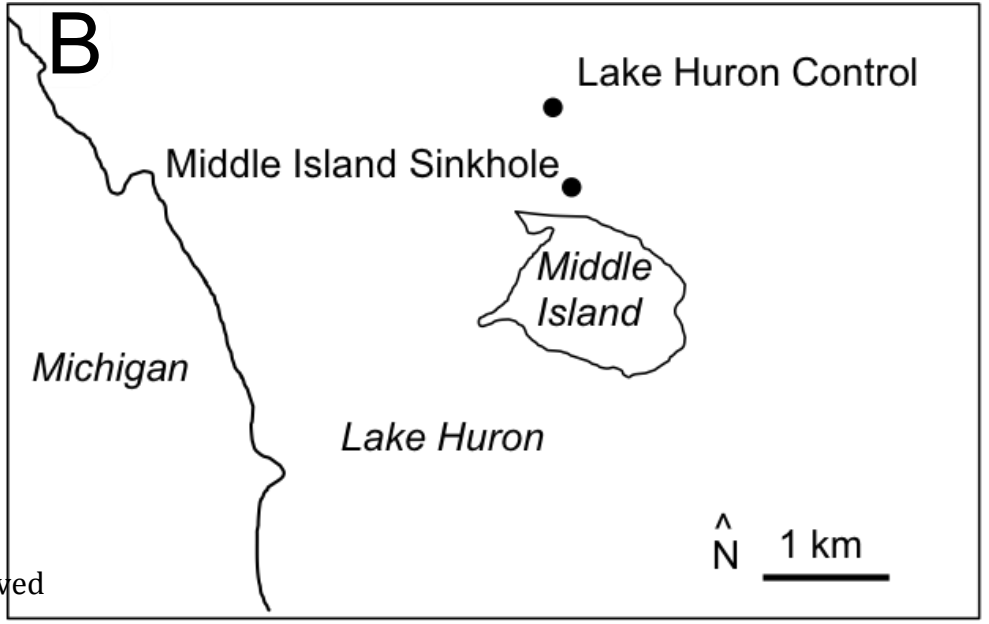

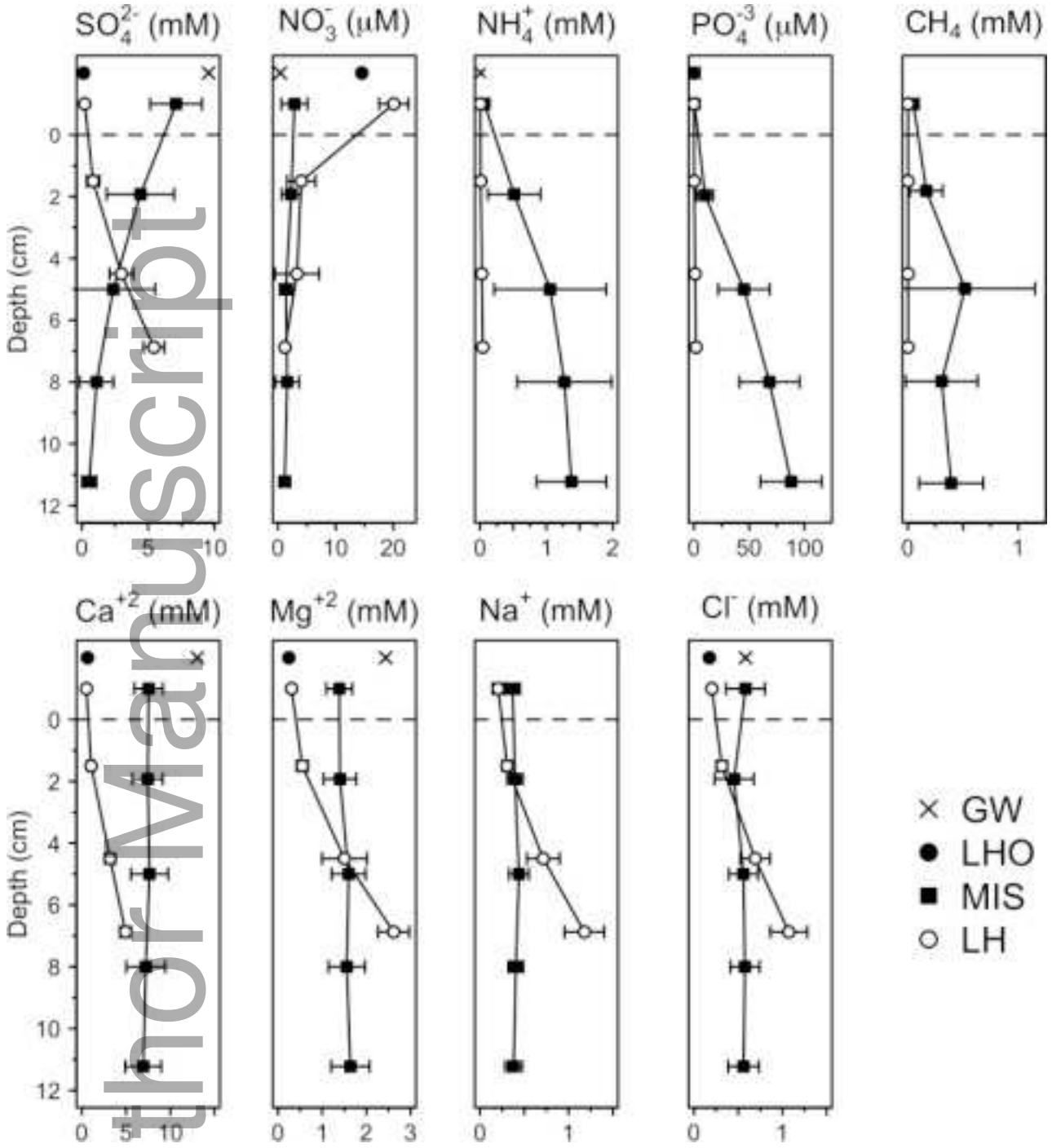

gbi_12215_f2.tiff

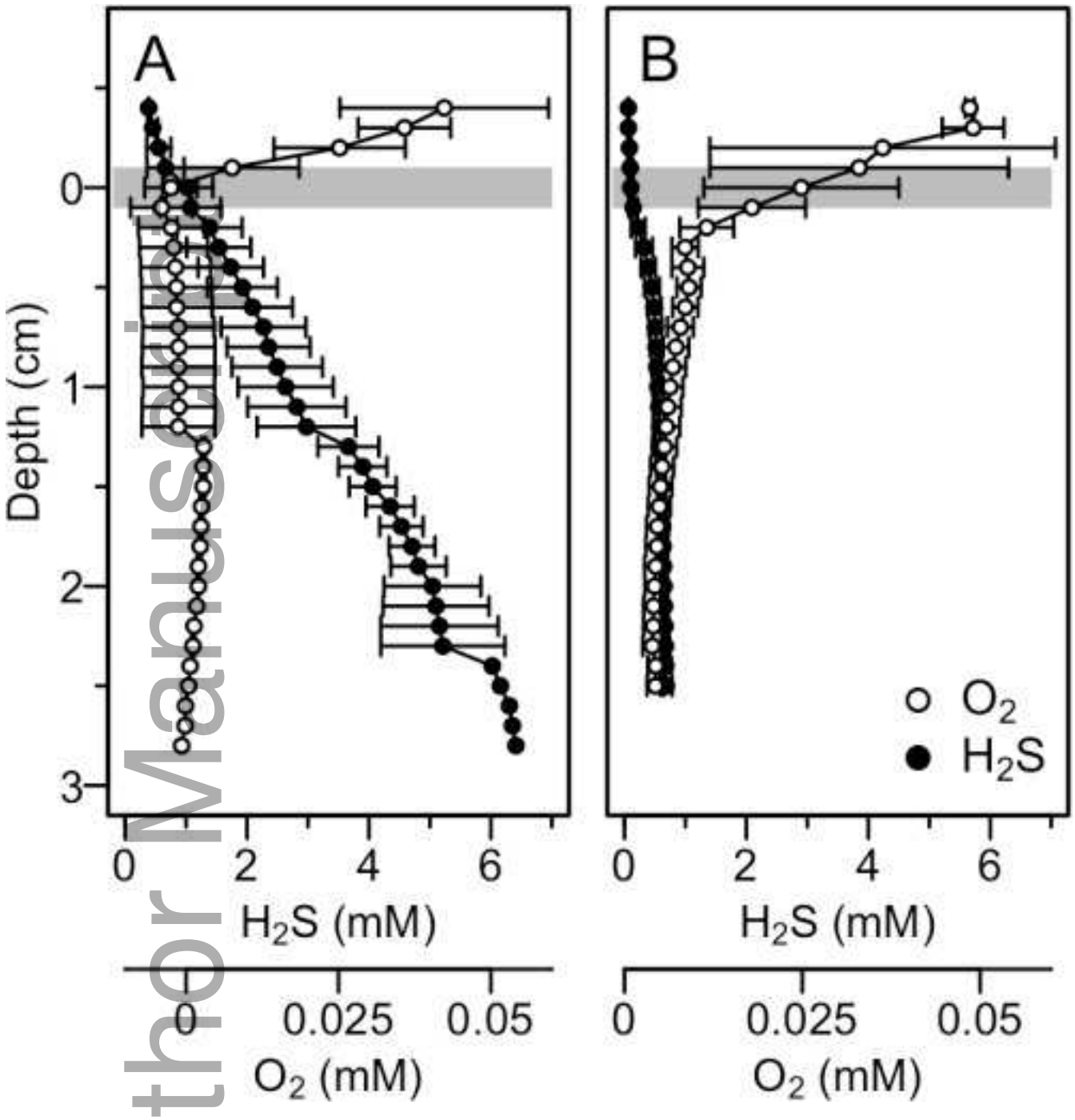

gbi_12215_f3.tiff

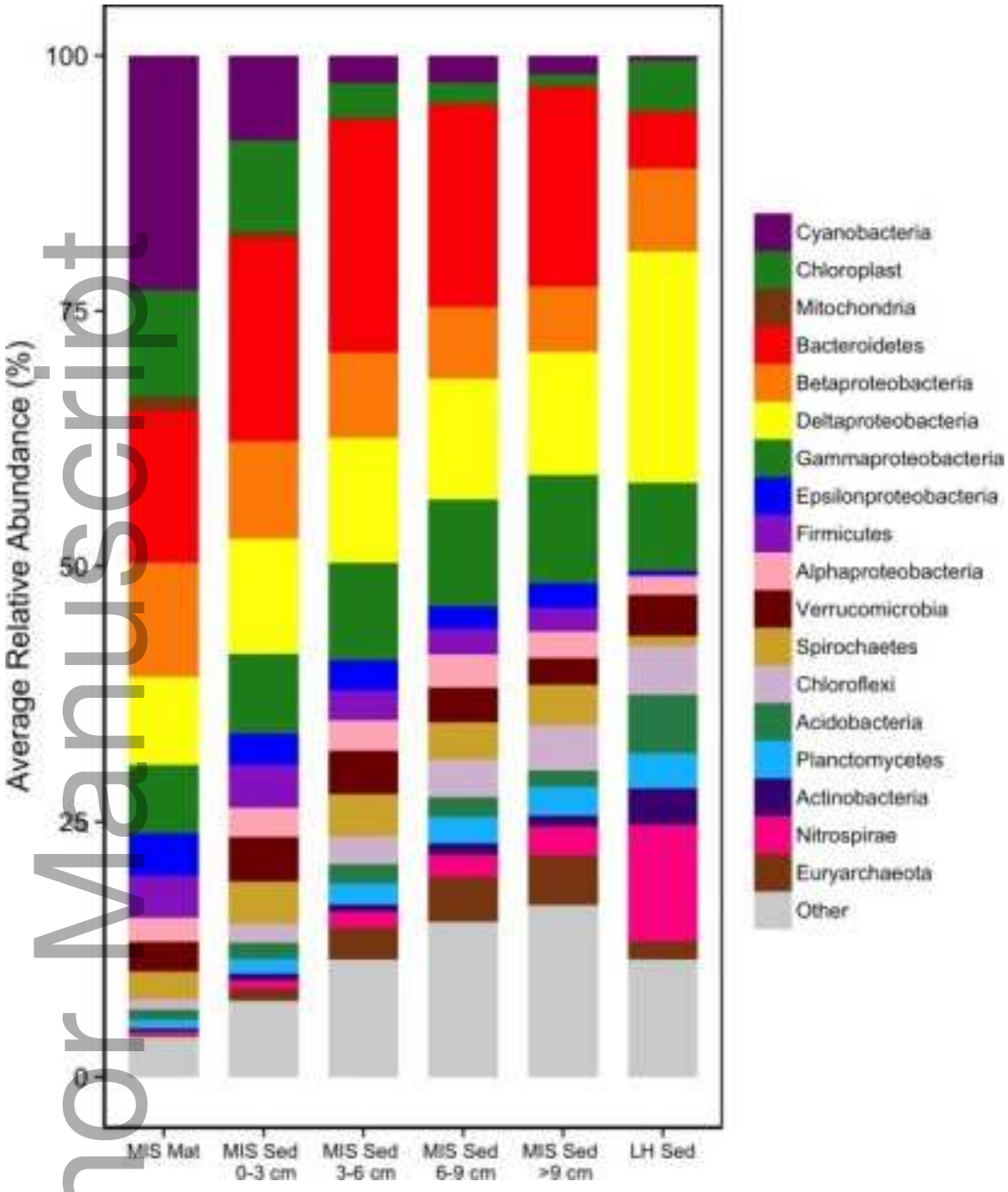

gbi_12215_f4.tiff

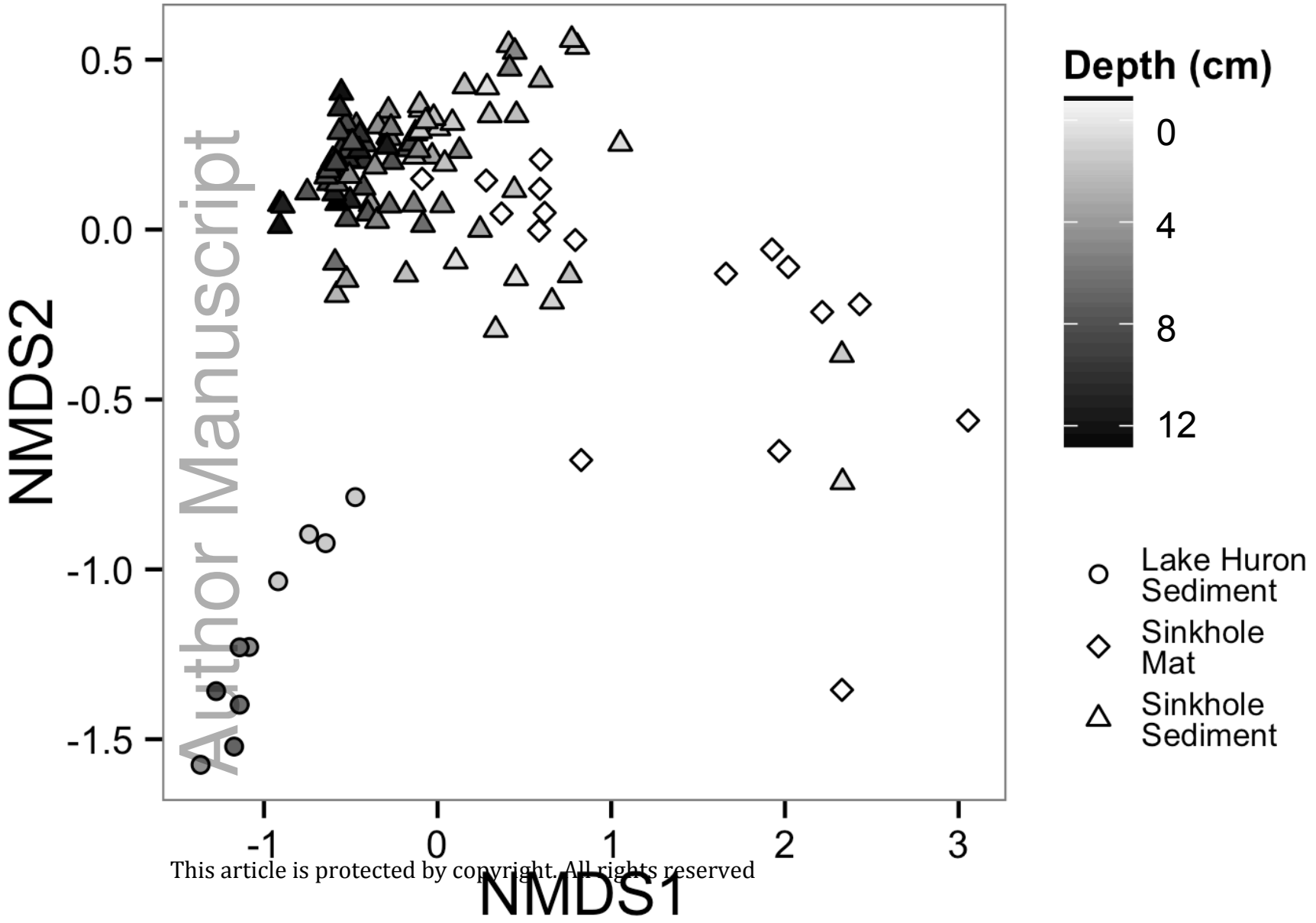

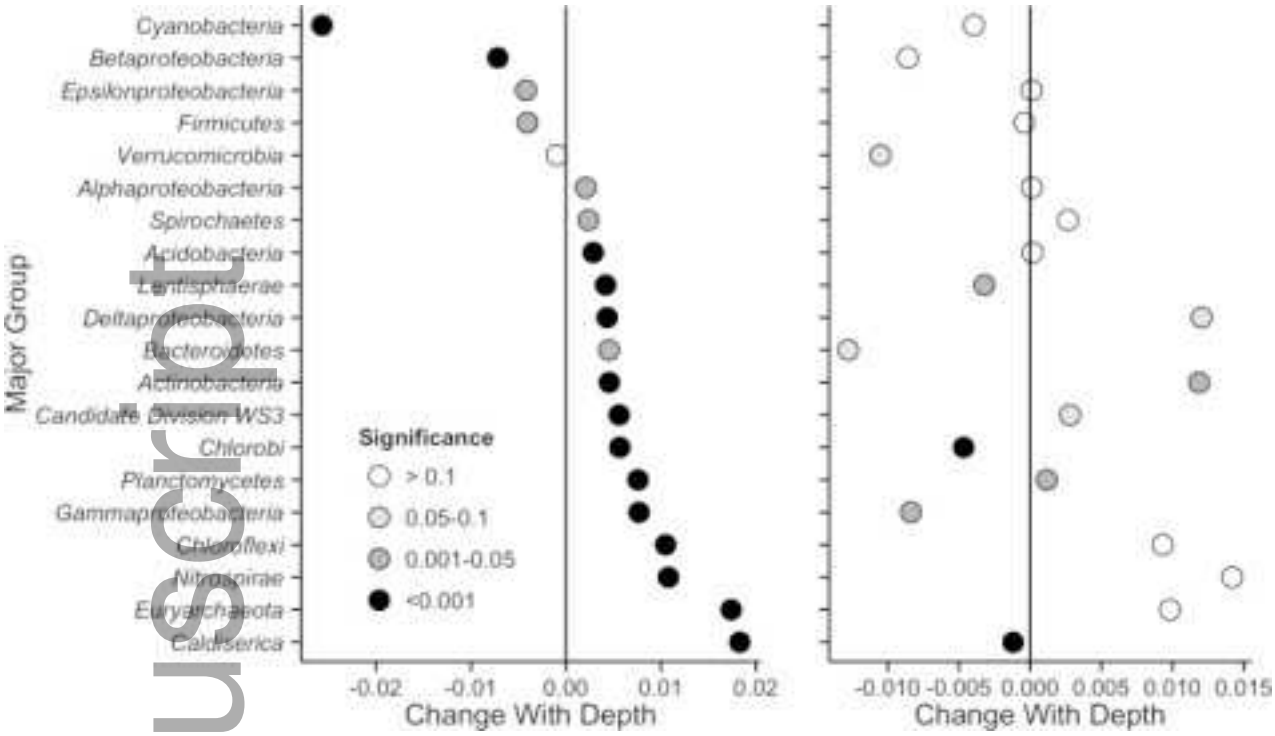

gbi_12215_f6.tiff

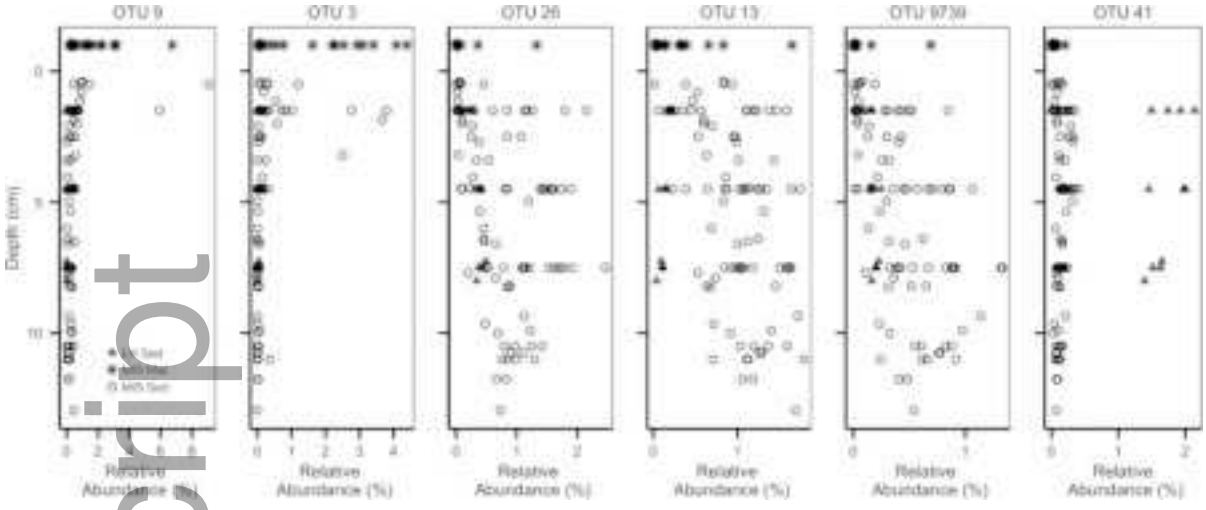

gbi_12215_f7.tiff